

Assessment of evidence against homogeneity in exhaustive subgroup treatment effect plots

Björn Bornkamp¹, Jiarui Lu², and Frank Bretz^{1,3}

¹Advanced Methodology and Data Science, Novartis Pharma AG, Basel, Switzerland

²Department of Biometrics, Vertex Pharmaceuticals Inc., Boston, MA, USA

³Institute of Medical Statistics, Center for Medical Data Science, Medical University of Vienna, Vienna, Austria

February 9, 2026

Abstract

Exhaustive subgroup treatment effect plots are constructed by displaying all subgroup treatment effects of interest against subgroup sample size, providing a useful overview of the observed treatment effect heterogeneity in a clinical trial. As in any exploratory subgroup analysis, however, the observed estimates suffer from small sample sizes and multiplicity issues. To facilitate more interpretable exploratory assessments, this paper introduces a computationally efficient method to generate homogeneity regions within exhaustive subgroup treatment effect plots. Using the Doubly Robust (DR) learner, pseudo-outcomes are used to estimate subgroup effects and derive reference distributions, quantifying how surprising observed heterogeneity is under a homogeneous effects model. Explicit formulas are derived for the homogeneity region and different methods for calculation of the critical values are compared. The method is illustrated with a cardiovascular trial and evaluated via simulation, showing well-calibrated inference and improved performance over standard approaches using simple differences of observed group means.

Keywords: causal inference; efficient influence function; funnel plot; subgroup analysis; subgroup identification; treatment effect heterogeneity.

1 Introduction

Subgroup analyses present significant challenges in biostatistics, particularly in clinical trials. Estimating treatment effects within subgroups is often unreliable due to limited sample sizes and multiplicity issues. This frequently leads to findings that fail to generalize beyond the observed data, as is often seen when initial subgroup findings are not replicated in subsequent trials [31, 3, 29, 22]. These challenges primarily affect exploratory subgroup analyses, whereas pre-specified analyses with adequate sample sizes and multiple testing strategies are generally more reliable [1].

In any clinical trial, some treatment effect heterogeneity will be observed. The key question is whether the observed heterogeneity is notable. One way to assess this is to frame the findings in the context of treatment effect homogeneity and investigate how likely the observed subgroup differences are under a model assuming homogeneous treatment effects. This can be achieved with a global interaction test, and several authors have emphasized its importance for

evaluating subgroup treatment effect heterogeneity in both univariate and multivariate settings [7, 23, 18, 30, 15, 9, 10]. Although interaction tests are widely used, clinical trials are not typically powered for them, as they are not of primary importance. Therefore, the resulting p-values should be interpreted with caution and not as strict binary decision rules.

Recently Muysers and others[20, 19] advocated an exhaustive display of subgroup treatment effects. Rather than focusing on a limited set of subgroups, as in a forest plot, they proposed plotting treatment effect estimates for all single- and multi-level subgroups against their respective sample sizes. Their aim was to efficiently calculate point estimates for multiple subgroups to explore those that may differ from the average treatment effects across all subgroups (i.e., the overall treatment effect). We refer to this display as exhaustive subgroup treatment effect plots, with subgroup size on the x-axis and subgroup treatment effect on the y-axis (see Figure 1 for an example). This graphical approach provides context by comparing subgroups of similar size, offering a comprehensive assessment rather than selective reporting. Importantly, the authors deliberately avoided inferential statistics such as p-values or confidence intervals, to prevent distracting attention from clinically meaningful subgroups. Instead, they recommend using these plots in research team discussions to assess treatment effect homogeneity or heterogeneity.

To further aid interpretation, we develop in this paper a computationally efficient method to derive homogeneity regions for the differences between subgroup treatment effects and the overall treatment effect, situating observed results within a model of homogeneous effects. More specifically, we apply the Doubly Robust (DR) learner[16] to generate pseudo-outcomes for the individual treatment effect of each patient, estimate subgroup treatment effects by averaging pseudo-outcomes within subgroups, and compute probabilities and thresholds from the underlying reference distribution. We interpret the resulting p-values not as binary decision rules, but as divergence p-values[13]. These quantify the compatibility of the observed data with a model of homogeneous treatment effects [8]. A large p-value indicates compatibility, whereas a small p-value suggests inconsistency between the data and the homogeneity model.

The remainder of this paper is structured as follows. Section 2 introduces a synthetic simulated data set mimicking data from a cardiovascular outcome trial to motivate our approach. Section 3 presents the proposed methodology. Section 4 evaluates its operating characteristics through simulation. Section 5 revisits the motivating example, and Section 6 concludes.

2 Case study

To illustrate the methods in this article, we use synthetic simulated data that mimic data from a cardiovascular outcome trial comparing three investigational doses against placebo. For the purpose of this paper, we focus on the comparison of the highest dose group against placebo for an exploratory outcome of interest, high-sensitivity C-reactive protein (hs-CRP), an inflammation marker that is measured three months post baseline. The dataset includes 3297 patients in the placebo group and 2194 in the highest dose group. Note that the sample size of this trial was determined for the primary time-to-event endpoint. The power to detect differences in hs-CRP is considerably higher than would typically be the case in analyses of treatment effect heterogeneity targeting the primary endpoint. This setting therefore provides greater opportunity to detect differences in treatment effects across subgroups compared to standard situations where treatment effect heterogeneity is explored for a primary endpoint.

For reasons of confidentiality, we use simulated data. We analyze the change from baseline in log-transformed hs-CRP values using a linear model adjusting for baseline log10-transformed hs-CRP, focusing on the highest dose versus placebo. This analysis yields a treatment effect estimate of -0.38 with a 95% confidence interval of $(-0.40, -0.36)$, corresponding to a reduction of approximately 59% in hs-CRP relative to baseline compared with placebo. Thus, a clear treatment effect is present in the data for this outcome.

In addition, we employ the exhaustive subgroup treatment effect plot[20]. As potential effect modifiers, we consider 19 baseline variables described in Table 3 in the Appendix A, most of which were pre-specified for subgroup analyses of the primary endpoint in the original study. Numerical baseline variables were categorized into tertiles. We consider all single-variable subgroups as well as two-variable cross-classifications, restricting to subgroups with at least 50 patients in both treatment and control arms. This results in a total of 1408 subgroups.

Figure 1 displays the treatment effect estimates of all these subgroups on the y-axis against subgroup size on the x-axis. As expected, the plot exhibits a funnel shape: smaller subgroups show greater variability in treatment effect estimates, whereas larger subgroups display reduced variability and converge toward the overall treatment effect estimate, reflecting greater overlap with the overall population. The R package *subscreen*[20, 19] provides an interactive version of such a plot, allowing users either to identify points corresponding to specific subgroups of interest or to click on points to reveal the associated subgroup. Such a display provides a useful overview of how treatment effects vary with baseline covariates.

As discussed in Section 1, the original approach does not provide a formal method to assess evidence against homogeneity. Nevertheless, we believe that such exploratory investigations can be further enhanced by considering how surprising the observed heterogeneity of certain subgroups is under a model of homogeneous treatment effects. Along the lines of Questions 3 and 4 posed by Stephen Senn[26], research teams may naturally ask the following questions based on an exhaustive subgroup treatment effect plot:

- (A) How heterogeneous are the treatment effects across all subgroups? To what extent is the observed heterogeneity consistent with the hypothesis that all subgroups share the same treatment effect?
- (B) Which subgroups exhibit larger or smaller treatment effects compared with the overall trial population?

We return to these questions in Section 5.

3 Methodology

Creating an exhaustive subgroup treatment effect plot requires calculating subgroup treatment effects for a potentially large number of subgroups, which can be computationally intensive if statistical models are fit separately for each subgroup. To address this challenge, we propose using pseudo-outcomes φ_i for the individual treatment effect of each patient i , based on a two-stage doubly robust estimator, known as the DR learner [16]. Subgroup treatment effects can then be estimated by averaging the pseudo-outcomes φ_i within each subgroup, reducing computational complexity from (potentially iterative) model fitting to simple averaging.

Assume independent and identically distributed samples $Z_i = (Y_i, A_i, X_i)$, where $Y \in \mathbb{R}$ denotes the outcome of interest, $A \in \{0, 1\}$ a binary treatment indicator, and $X \in \mathbb{R}^d$ the covariates. The intuition behind pseudo-outcomes in the DR learner is to create a new outcome that combines information from both a propensity score model $\pi(x) = \mathbb{P}(A = 1|X = x)$ (the probability of receiving treatment given the covariates) and an outcome model $\mu_a = \mathbb{E}(Y|X = x, A = a)$ (the expected outcome for a patient given their covariates and treatment). Assuming for now that $\pi(x)$, $\mu_0(x)$, and $\mu_1(x)$ are known, the pseudo-outcomes are constructed as [16]

$$\varphi(Z_i) = \mu_1(X_i) - \mu_0(X_i) + \frac{A_i - \pi(X_i)}{\pi(X_i)(1 - \pi(X_i))} (Y_i - \mu_{A_i}(X_i)).$$

The $\varphi(Z_i)$ are again independent and identically distributed with $Var(\varphi(Z_i)) = \sigma^2$ for all i . Furthermore, the semiparametric most efficient estimate of the average treatment effect for the overall population is simply the average of the $\varphi(Z_i)$ [14, 17]. Similarly, the most efficient effect estimate for a given subgroup is the average of the $\varphi(Z_i)$ within that subgroup. In what follows we will omit Z_i and simply write φ_i for $\varphi(Z_i)$.

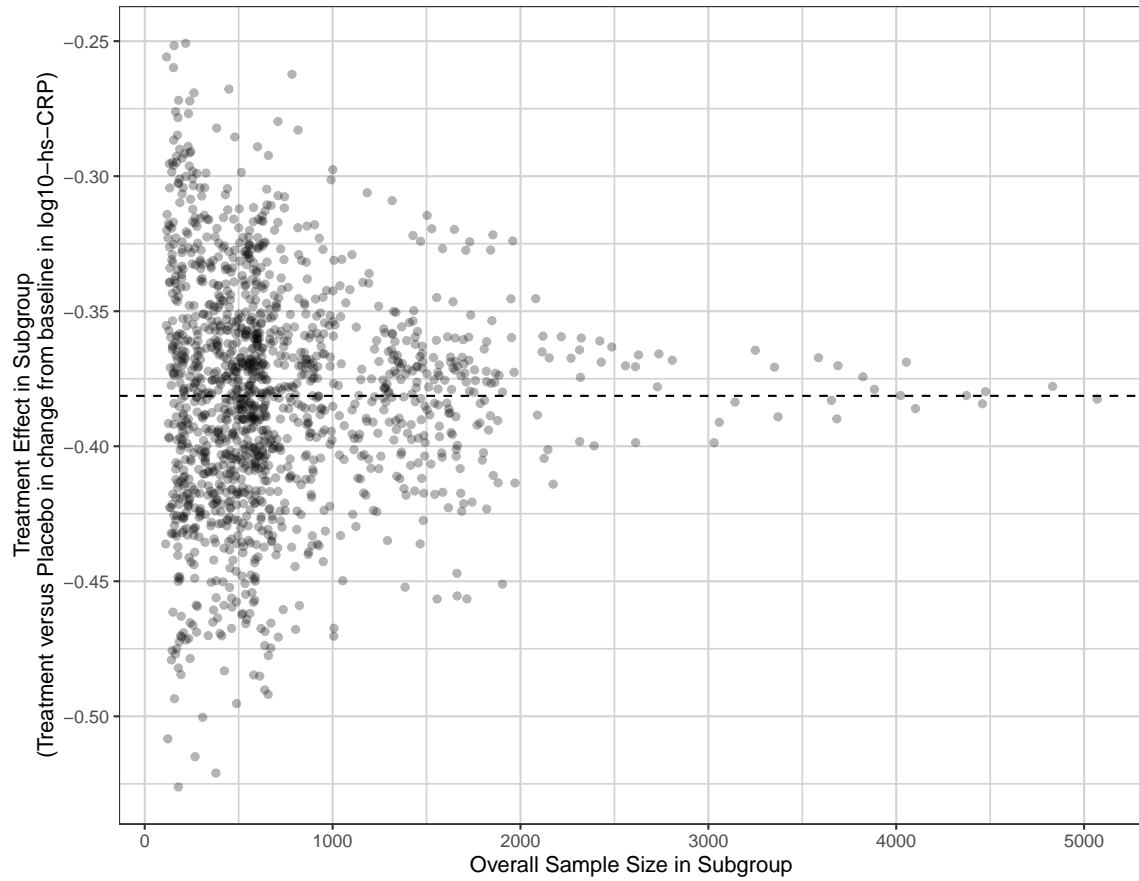


Figure 1: Exhaustive subgroup treatment effect plot, showing 1408 one-level or two-level subgroup treatment effects. The dashed line corresponds to the overall treatment effect estimate.

Next, consider index sets \mathcal{S}_j containing the patients in subgroup $j \in \{1, \dots, k\}$, where k denotes the total number of subgroups. Let $N_j = |\mathcal{S}_j|$ denote the size of subgroup j , and $N = |\bigcup_j \mathcal{S}_j|$ the total sample size. An estimator of the treatment effect in subgroup j is given by $\hat{\delta}_j = \frac{1}{N_j} \sum_{i \in \mathcal{S}_j} \varphi_i$ and of the overall treatment effect by $\hat{\delta} = \frac{1}{N} \sum_i \varphi_i$. Motivated by Questions (A) and (B) in Section 2, we assess the k estimated treatment effect differences $\hat{\Delta}_j = \hat{\delta}_j - \hat{\delta}$ and determine whether the magnitude of $\hat{\Delta}_j$ is large relative to its variability under the assumption of no treatment effect heterogeneity.

Let $T_j = \hat{\Delta}_j / \sqrt{V_j}$, where V_j denotes the variance of $\hat{\Delta}_j$. More precisely, we note that $Var(\hat{\delta}_j) = Var\left(\frac{1}{N_j} \sum_{i \in \mathcal{S}_j} \varphi_i\right) = \sigma^2/N_j$ and $Cov(\hat{\delta}_j, \hat{\delta}) = \frac{1}{N N_j} Cov\left(\sum_{i \in \mathcal{S}_j} \varphi_i, \sum_i \varphi_i\right) = \frac{1}{N N_j} \sum_{i \in \mathcal{S}_j} Var(\varphi_i) = \sigma^2/N$. Thus, the variance V_j can be estimated as $\hat{V}_j = Var(\hat{\delta}_j - \hat{\delta}) = Var(\hat{\delta}_j) - 2Cov(\hat{\delta}_j, \hat{\delta}) + Var(\hat{\delta}) = \sigma^2 (N_j^{-1} - N^{-1})$.

To assess consistency of the observed heterogeneity with the model that all subgroups have the same treatment effect (Question A), we consider the maximum statistic $T_{\max} = \max_j |T_j|$ and compute the divergence p-value $p = 1 - F(T_{\max})$, where F denotes the reference distribution function under the assumption of homogeneity. We interpret this p-value as a measure of the dataset's discrepancy from what would be expected under a model of no treatment effect heterogeneity [13]: a small p indicates inconsistency with the treatment effect homogeneity assumption in the model used to derive the reference distribution.

Additionally, we can assess which subgroups have a differential (larger or smaller) treatment effect compared to the overall trial population (Question B) by computing individual divergence p-values $p_j = 1 - F(|T_j|)$, with F as defined above. We can also construct γ -homogeneity regions for the treatment effect differences by plotting $\hat{\delta} \pm q_\gamma \sigma \sqrt{N_j^{-1} - N^{-1}}$ as a function of subgroup size N_j , where $q_\gamma = F^{-1}(\gamma)$. Hence when the subgroup size (N_j) approaches N , the width of this interval, as expected, approaches 0. Under the model of no treatment effect heterogeneity, the differences between subgroup treatment effects and the overall treatment effect will all fall within the γ -homogeneity region with probability γ . In other words, whenever $T_{\max} > q_\gamma$, at least one subgroup will fall outside the γ -homogeneity region.

We now discuss how to compute probabilities for the reference distribution F . Assuming for now that σ and φ_i are known, we note that T_j is asymptotically standard normal, $T_j \sim N(0, 1)$. The random variables $\{T_1, \dots, T_k\}$ are jointly asymptotically multivariate normal with correlation matrix $R = (\rho_{ij})_{ij}$, where

$$\rho_{ij} = \left(\frac{N_{ij}}{N_i N_j} - \frac{1}{N} \right) \Bigg/ \sqrt{\left(\frac{1}{N_i} - \frac{1}{N} \right) \left(\frac{1}{N_j} - \frac{1}{N} \right)},$$

see Appendix B for details. Accordingly, we can calculate p using numerical integration as implemented in, for example, the *mvtnorm* package in R [11]. If the total number of subgroups k is large, numerical integration may be infeasible. In such cases, one may rely on approximations to the multivariate normal probability integral that consist of combinations of lower dimensional problems based on approximations to Boole's formula. The most widely known of these approximations is the inequality by Bonferroni[2]. Alternatively, we can approximate the reference distribution F using a permutation approach. Specifically, we permute the φ_i values while keeping subgroup indicators fixed (Algorithm 1). For each of N_{perm} permutations, we compute $T_{j,\ell}$ for subgroup j , and then calculate the maximum statistic $T_{\max,\ell} = \max_j |T_{j,\ell}|$, $\ell = 1, \dots, N_{\text{perm}}$. Since only the φ_i are permuted, the resulting collection $\{T_{\max,\ell}\}$ approximates the distribution of F . The quantity $q_\gamma = F^{-1}(\gamma)$ used in defining the γ -homogeneity region can then be estimated as the γ -quantile of $\{T_{\max,\ell}\}$, $\ell = 1, \dots, N_{\text{perm}}$.

So far, we have assumed φ_i and σ to be known. In practice, both must be estimated. We adapted Algorithm 1 from Kennedy[16] to construct $\hat{\varphi}_i$ for each patient i using a cross-fitting procedure, following the implementation details provided in Algorithm 1 of Sechidis and others[25]. The oracle property of pseudo-outcomes has been discussed extensively in the literature [16, 4, 6]. Under the stated conditions, Theorem 2 of Kennedy[16] shows that $\hat{\varphi}_i$ is a consistent estimator of φ_i . It also establishes that the error bound of the DR learner is at most the product of the

Algorithm 1 Permutation approach for computing probabilities for the reference distribution F

Input Number of permutations N_{perm} ; k pre-specified subgroups represented by index sets \mathcal{S}_j , $j \in \{1, \dots, k\}$; pseudo-outcomes φ_i ; variance σ^2 .

Output Empirical distribution of the maximum statistic T_{\max} .

for $\ell = 1, \dots, N_{perm}$ **do**

- Step 1: Permute the φ_i .
- for** $j = 1, \dots, k$ **do**

 - Step 2: Compute $T_{j,\ell}$ based on subgroup j and the ℓ -th permuted data.

- end for**
- Step 3: Compute $T_{\max,\ell} = \max_j |T_{j,\ell}|$ for the ℓ -th permuted data.

end for

Step 4: Estimate the γ -quantile of the reference distribution F of the maximum statistic T_{\max} , q_γ , by taking the γ -quantile of $\{T_{\max,\ell}\}$, $\ell = 1, \dots, N_{perm}$.

errors in the propensity score and regression estimators, which implies a faster rate of convergence compared to those of $\pi(x)$, $\mu_0(x)$, or $\mu_1(x)$. These results indicate that φ_i and σ can be replaced by their estimates without altering the key statistical properties described in this section. This will also be demonstrated in the simulation study in Section 4.

One might question the advantage of employing individual pseudo-outcomes, φ_i , for estimating subgroup treatment effects rather than relying on simple differences in group means across subgroups. A key limitation of using raw group means, particularly within small subgroups, is the potential for imbalances in important baseline covariates between treatment groups. Such imbalances can reduce the efficiency of subgroup-specific estimates. In contrast, the pseudo-outcomes φ_i incorporate baseline covariate information and can therefore be regarded as a form of covariate adjustment that enhances efficiency. This aspect will also be evaluated in the simulation study.

4 Simulation study

This section evaluates the proposed approach through a simulation study. We describe the aims of the study, the data-generating mechanisms with their assumptions and scenarios, the methods being compared, the performance metrics used to evaluate statistical operating characteristics, and a graphical summary of the statistical performance of the methods, based on the simulation results.

4.1 Aims

The aim of the simulation study is to compare the repeated sampling properties of the approach proposed in Section 3 for calculating p-values and γ -homogeneity regions under homogeneous and heterogeneous effect scenarios, and to contrast it with a simpler approach that does not use pseudo-outcomes.

4.2 Data-generating mechanisms

We adopt the simulation setup implemented in the R package *bencthm* [27], introduced in [28] and further extended in [5]. We assume a two-arm randomized trial with $N = 500$ patients. The treatment indicator A_i for patient i is

Table 1: Data-generating models. Here, $a \vee b$ denotes ‘a or b’, $a \wedge b$ denotes ‘a and b’, $I(\cdot)$ is the indicator function, $\Phi(\cdot)$ is the cumulative distribution function of the standard normal distribution, and s is a scaling factor depending on the data generating model; see the *benchtm* package for details.

Scenario	Model equation
1	$f(X_i, A_i) = s \times (0.5I(X_{1,i} = Y) + X_{11,i}) + A(\beta_0 + \beta_1 \Phi(20(X_{11,i} - 0.5)))$
2	$f(X_i, A_i) = s \times (X_{14,i} - I(X_{8,i} = N)) + A(\beta_0 + \beta_1 X_{14,i})$
3	$f(X_i, A_i) = s \times (I(X_{1,i} = N) - 0.5X_{17,i}) + A(\beta_0 + \beta_1 I((X_{14,i} > 0.25) \wedge (X_{1,i} = N)))$
4	$f(X_i, A_i) = s \times (X_{11,i} - X_{14,i}) + A(\beta_0 + \beta_1 I((X_{14,i} > 0.3) \vee (X_{4,i} = Y)))$

generated by permuting a vector with 250 zeros and 250 ones. The mean response is

$$f(A_i, X_i) = f_{\text{prog}}(X_i) + A_i(\beta_0 + \beta_1 f_{\text{pred}}(X_i)), \quad (1)$$

where $f_{\text{prog}}(X_i)$ represents the prognostic component and $f_{\text{pred}}(X_i)$ the predictive component, based on baseline covariates X_i . For the purpose of this simulation study, we restrict attention to continuous response variables, with $Y_i = f(X_i, A_i) + \epsilon_i$, where $\epsilon_i \sim N(0, 1)$. The covariates X_i are 30-dimensional and generated to mimic a realistic scenario [28]. Table 1 summarizes the four data-generating models considered. These models include step-like (Scenario 1) and linear (Scenario 2) functions, as well as predictive effects defined by multiple covariates (Scenarios 3 and 4).

The parameters β_0 and β_1 are jointly chosen to achieve a power of 0.5 for an unadjusted Z-test of the overall treatment effect. This reflects a realistic clinical trial setting, where the observed effect is smaller than anticipated at the design stage. In such situations, there may be interest in exploring covariates that modify the treatment effect and identifying subgroups with potentially larger effects.

We determined the value β_1^* to ensure 80% power for the interaction test of $H_0 : \beta_1 = 0$ versus $H_1 : \beta_1 \neq 0$ under the true model (1), at a significance level of 0.1. In our simulation study, we consider $\beta_1 = 0$ and $\beta_1 = 2\beta_1^*$ to represent scenarios of treatment effect homogeneity and heterogeneity, respectively. For $\beta_1 = 2\beta_1^*$, there is thus a high probability of detecting effect modification if $f_{\text{prog}}(X)$ and $f_{\text{pred}}(X)$ were known.

To generate candidate subgroups based on the 30 baseline covariates X_i , numerical variables are categorized into three groups using tertiles of their distributions, while categorical variables define subgroups by each category. In addition, these univariate subgroups are combined with an ‘and’ operator. Subgroups with fewer than 10 patients in either treatment arm are excluded. This leads to approximately 3200–3300 subgroups, depending on the simulated covariates. The numerical integration approach based on the multivariate normal distribution described in Section 3 is computationally slow in this dimensionality. We therefore also consider a stricter requirement of at least 60 patients per treatment arm in each subgroup, reducing the number of investigated subgroups to 190–230. Note that the subgroup definitions are not informed by the true predictive models. For instance, the ideal subgroup in Scenario 1 would involve splitting X_{11} at 0.5, whereas in Scenario 4 it would combine X_4 and X_{14} with an ‘or’ operator. Since all methods are equally affected, this does not limit the conclusions of this simulation study; rather, it reflects how such analyses would be conducted in practice.

4.3 Methods

We compare the three methods described in Section 3 to compute p-values of the maximum statistic T_{\max} and the associated thresholds q_γ used to derive γ -homogeneity regions for treatment effect differences: numerical integration,

Bonferroni approximation, and the permutation approach described in Algorithm 1. All three methods rely on the pseudo-outcomes φ_i , estimated using a five-fold cross-fitting procedure as outlined in Algorithm 1 of Sechidis and others[25]. For estimation of the mean functions μ_0 and μ_1 in each cross-validation fold, we use an ensemble method implemented in the R package *SuperLearner* [21], with LASSO and random forest as base learners. In our simulation setting, the LASSO model is correctly specified for μ_0 , but for μ_1 only the random forest can reasonably approximate the true functions. For the propensity score model, we use the known randomization probabilities.

The permutation approach is conducted with $N_{perm} = 500$ permutations. For the multivariate normal integration approach, we use the R package *mvtnorm* with default control parameters. Since the correlation matrix of the test statistics (Section 3) is in general not positive definite, we apply the *Matrix::nearPD* function to compute the nearest positive definite correlation matrix. As discussed earlier, due to computational complexity the multivariate integration approach is applied only in the scenario with fewer subgroups (60 patients per arm within each subgroup).

In addition to the approaches based on pseudo-outcomes, we consider an approach using the simple differences in group means. Let $\bar{Y}_{a,j}$ denote the mean and $n_{a,j}$ the number of patients on treatment a in subgroup \mathcal{S}_j , and let \bar{Y}_a and n_a denote the corresponding overall quantities. The test statistic in subgroup \mathcal{S}_j is given by $T_j = \frac{\bar{Y}_{1,j} - \bar{Y}_{0,j} - (\bar{Y}_1 - \bar{Y}_0)}{s_j}$, where $s_j = \tau \sqrt{1/n_{1,j} + 1/n_{0,j} - 1/n_1 - 1/n_0}$, with τ estimated as the standard deviation of the observations Y_i . Quantiles of the distribution of the maximum statistic are approximated using the Bonferroni method.

4.4 Performance measures

As performance measures, we consider the repeated sampling distribution of the p-value. Specifically, this is the probability approximated by each method that T_{\max} exceeds the observed value of the maximum statistic.

- Under homogeneity, we present the empirical distribution function of the obtained p-values, which should closely approximate the uniform distribution on the unit interval, $U([0, 1])$, if they constitute valid p-values [12].
- Under heterogeneity, we display density plots of the p-values, together with the proportion of p-values less than 0.1 to evaluate the ability of each method to detect departures from homogeneity.

4.5 Results

Simulations were performed with 2000 repetitions. Figure 2 displays the empirical distribution function of the p-values, along with the diagonal line corresponding to the $U([0, 1])$ distribution. For scenarios with at least 10 observations in both treatment and control arms, the permutation approach closely follows the $U([0, 1])$ distribution. The two Bonferroni-type approaches lie consistently below the diagonal (hence conservative) and do not follow the $U([0, 1])$ distribution, showing a spike at 1. This is undesirable, as it makes the resulting p-values more difficult to interpret. The results for 60 observations per arm are similar; this case also includes the integration-based approach, which is essentially indistinguishable from the permutation approach and likewise closely follows the $U([0, 1])$ distribution.

Figure 3 shows vertical density plots of the distribution of p-values under the scenario with $\beta_1 = 2\beta_1^*$, where treatment effect heterogeneity is present (the corresponding plots under homogeneity are provided in Figure 6 in Appendix C). The densities under the permutation and integration-based approaches are very similar. Compared to the Bonferroni-based approaches, the permutation and integration-based methods yield smaller median p-values (indicated by horizontal lines) and are generally shifted toward lower values. Between the two Bonferroni-based methods, the version using pseudo-outcomes performs slightly better, likely because the construction of pseudo-outcomes implicitly incorporates covariate adjustment.

Figure 4 summarizes the proportion of p-values less than 0.1, where 0.1 is used as an illustrative threshold. Under homogeneity, all approaches yield probabilities of about 0.1 or less, as expected from Figure 2. Under heterogeneity,

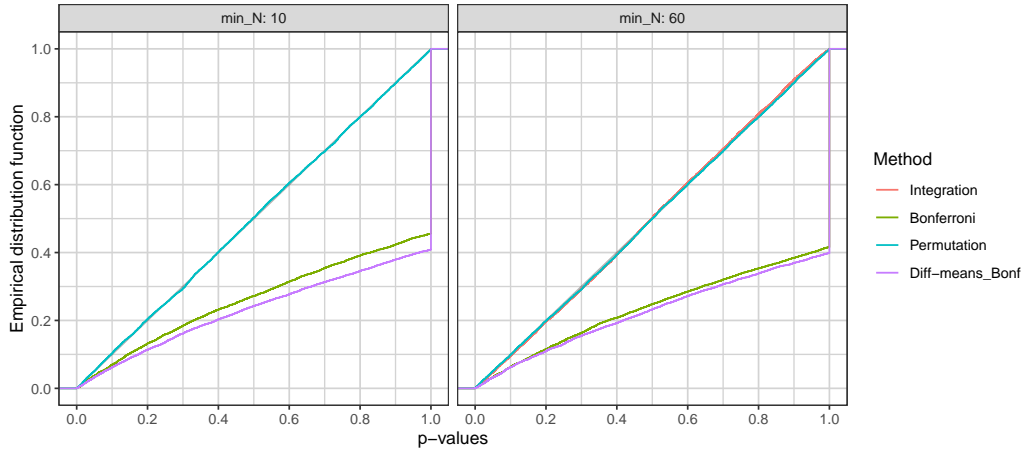


Figure 2: Empirical distribution function of p-values under no treatment effect heterogeneity. Results are pooled across the four scenarios from Table 1, thus resulting in 8000 simulations.

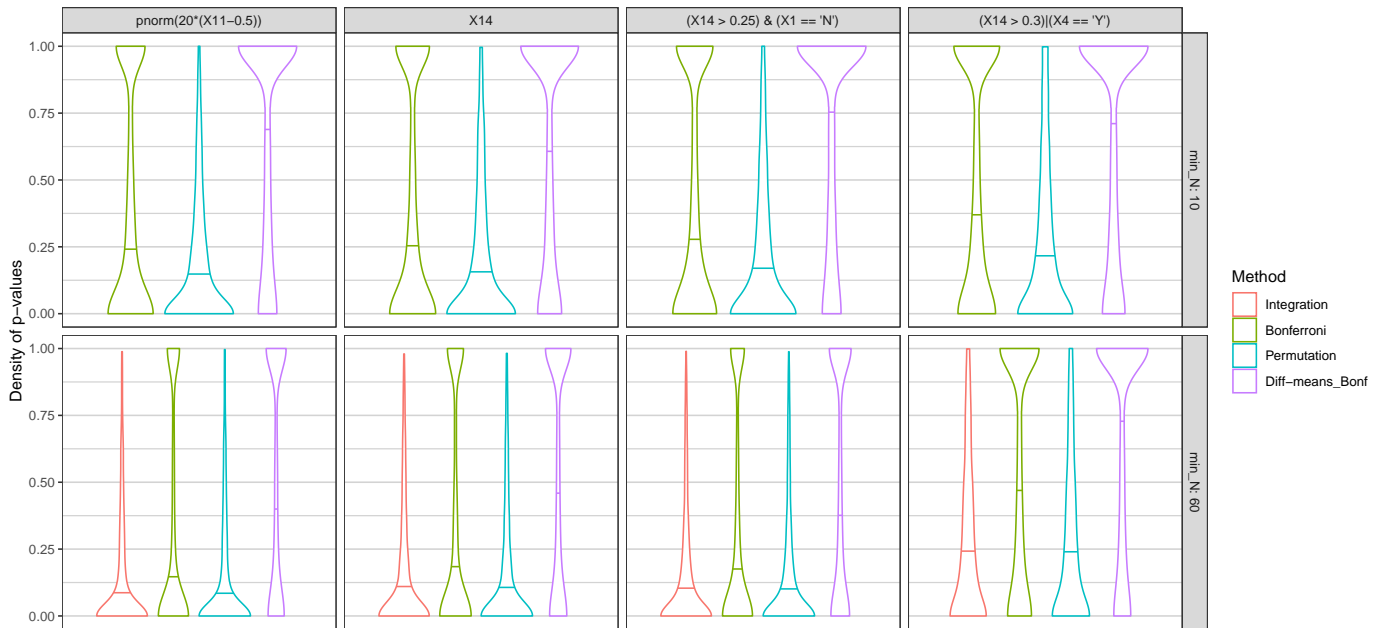


Figure 3: Distribution of p-values under treatment effect heterogeneity, shown as density plots. Horizontal lines indicate the median.

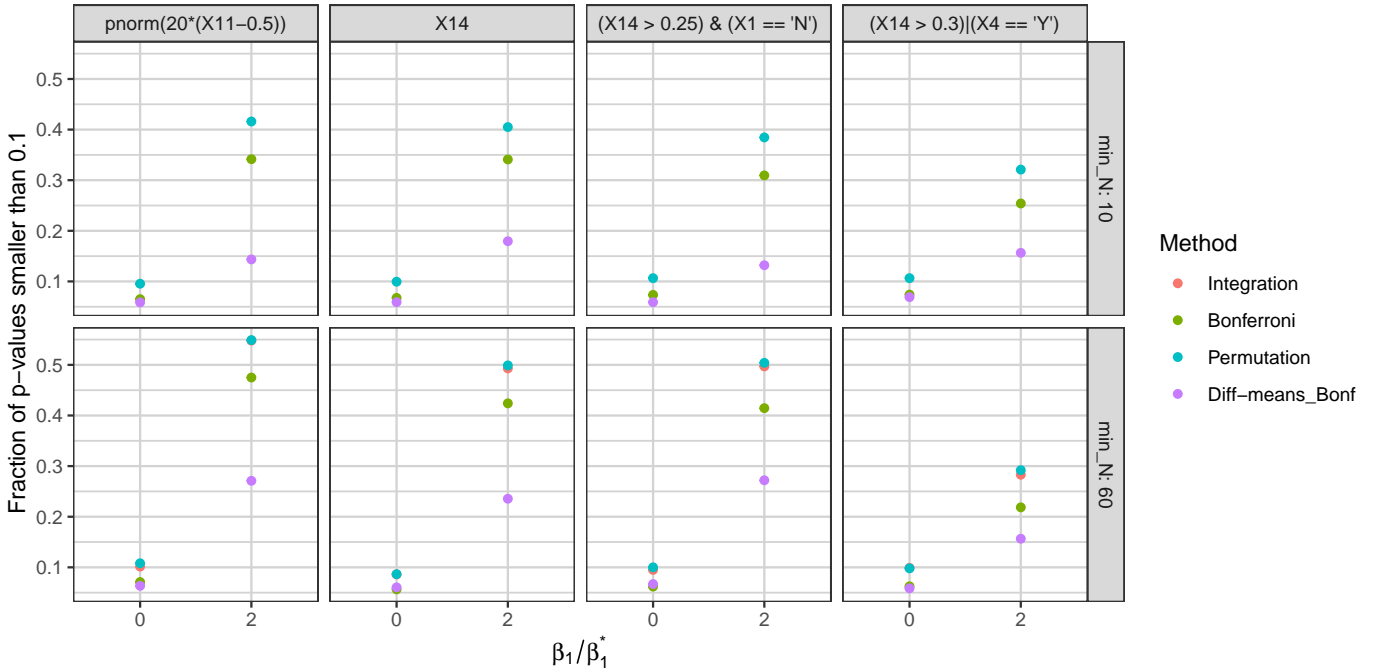


Figure 4: Proportion of p-values less than 0.1 across all scenarios.

the permutation approach outperforms the Bonferroni-based methods in the setting with at least 10 patients per arm and subgroup. For the setting with at least 60 patients per arm and subgroup, all methods show increased probabilities, likely due to reduced multiplicity when fewer subgroups are investigated. Overall, the results confirm that the integration- and permutation-based approaches perform very similarly and better than the Bonferroni-based methods. Among the Bonferroni-based approaches, the version based on pseudo-outcomes consistently outperforms the one based on simple subgroup means.

5 Example revisited

In this section, we revisit the example from Section 2. The pseudo-outcomes for the treatment effect were generated using an ensemble approach with the R package *SuperLearner*. For each treatment arm, we applied 10-fold cross-fitting with LASSO and random forest as base learners. The resulting out-of-fold predictions for $\mu_0(X_i)$ and $\mu_1(X_i)$, together with the true propensity scores, were used in the equation for the pseudo-outcomes. Both the permutation approach and the Bonferroni approximation were then applied to derive the γ -homogeneity intervals described in Section 3.

Figure 5 shows the resulting homogeneity regions in terms of (binary) surprise values [8, 13]. A surprise value (or S-value) is defined as $S = -\log_2(p)$ and can be interpreted as the amount of information, measured in bits, against the homogeneity assumption. For example, $S = 1$ corresponds to one bit of information, equivalent to the evidence provided by a single fair coin toss coming up heads; $S = 10$ corresponds to about ten bits of information, which is substantially stronger evidence. Larger S-values therefore indicate results that are more surprising under the homogeneity model and thus stronger evidence against it. The homogeneity regions in Figure 5 are displayed for $S = 2, 5$, and 10 , roughly corresponding to $\gamma = 0.75, 0.97$, and 0.999 , respectively. As expected, intervals are wider for smaller subgroups and gradually narrow as sample size increases. When the subgroup size equals the overall sample size, the lower and upper bounds coincide.

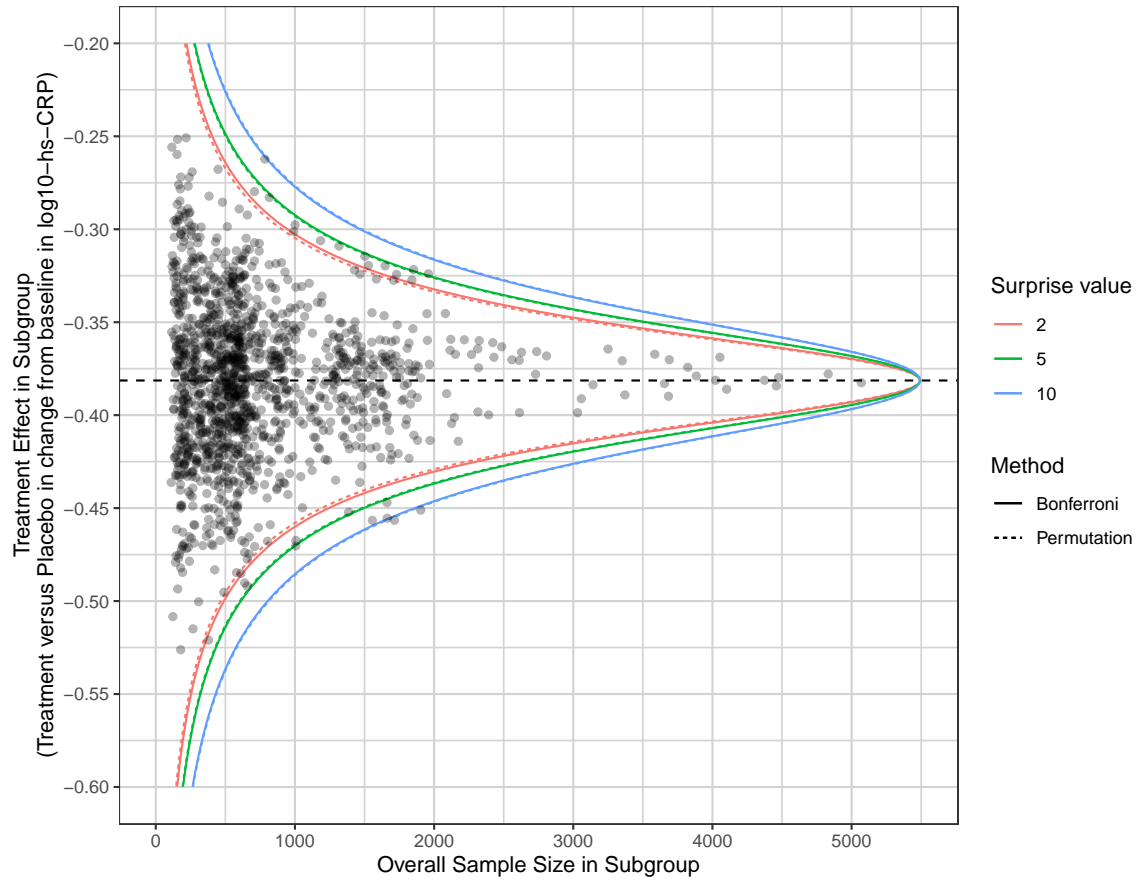


Figure 5: Exhaustive subgroup treatment effect plot, showing 1408 one-level or two-level subgroup treatment effects. The dashed line corresponds to the overall treatment effect estimate.

The intervals derived from the permutation and Bonferroni approaches are closely aligned, although the permutation-based intervals are narrower, reflecting the conservative nature of the Bonferroni approximation. The difference between the quantile curves decreases for larger quantiles. We attribute this to the limitations of the normal approximation used in the Bonferroni approximation: for extreme critical values (e.g., a surprise value of 10), the normal tails may underestimate the empirical tails of the test statistic distribution, particularly when small subgroups are included in the analysis.

Some subgroups in Figure 5 cross the line associated with a surprise value of 10, indicating strong evidence of treatment effect heterogeneity. Table 2 lists the five subgroups with the largest absolute maximum statistics in the simulated data. In practice, findings such as those in Table 2 would need to be examined for clinical relevance and in the context of external evidence (e.g., whether independent data exist that corroborate these results) and likely trigger further discussions.

Table 2: Five subgroups with the largest absolute test statistics

Subgroup	N (trt)	N (ctrl)	Trt. effect	$ T $
BMI > 32	767	1137	-0.45	5.13
No GOUT & BMI > 32	679	1036	-0.46	5.12
RACE = "White" & BMI > 32	675	988	-0.46	4.93
11 < BMI < 28 & 0.1 < LOGHDL \leq 0.59	314	470	-0.26	4.91
BMI > 32 & ETHNIC = "Not hispanic or latino"	622	934	-0.46	4.78

6 Discussion

Exploration of treatment effect heterogeneity is a critical component in clinical trials, as it may suggest subgroups of patients who benefit more or less from treatment. Exhaustive subgroup treatment effect plots provide an intuitive and comprehensive visualization for such exploratory analyses. In this paper, we developed a computationally feasible method to derive homogeneity regions for treatment effect differences, enabling systematic and interpretable summaries across large numbers of subgroups. This approach balances the need for rigorous statistical assessments in exploratory settings by considering how surprising the observed heterogeneity of certain subgroups is under a model of homogeneous treatment effects.

We interpret p-values as divergence p-values[13], which quantify the degree of incompatibility between the observed data and what would be expected under a model of no treatment effect heterogeneity. Unlike conventional interpretations of decision p-values, which are tied to thresholds for binary decisions, divergence p-values serve as graded measures of evidence. They can be further expressed as surprise values ($S = -\log_2(p)$), representing the amount of information in bits against a model of homogeneous treatment effects. For example, $S = 1$ corresponds to the evidence of a single coin toss, while $S = 10$ indicates substantially stronger evidence. For practical applications, research teams may find surprise values useful for communication, as they translate the strength of evidence into an intuitive scale that avoids the pitfalls of rigid dichotomization.

The R package *subscreen* provides an interactive graphical user interface for subgroup analysis [20, 19]. Such interactive displays allow users either to identify points corresponding to specific subgroups of interest or to click on points to determine which subgroup they represent. This functionality is valuable for obtaining an overall impression of how treatment effects vary with baseline covariates. A natural extension would be to enhance such interfaces with

functionality for displaying γ -homogeneity regions and surprise values as introduced in this paper, thereby combining interactivity with rigorous statistical calibration.

We compared several methods for constructing homogeneity regions in this paper. The approaches using numerical integration or permutation based on pseudo-outcomes for the treatment effect perform well across the scenarios considered. These approaches lead to uniformly distributed p-values under the scenario of homogeneity, which provides easier interpretation compared, for example, to the Bonferroni-based approaches. They also appear to detect deviations from homogeneity more often when such deviations exist. The permutation approach is computationally more expensive than Bonferroni but less involved than the integration approach. Overall, the permutation approach provides the most convincing performance in our simulations.

In this paper we utilized the difference in conditional means as the treatment effect measure of interest. Whether or not treatment effect heterogeneity exists and the extent of such heterogeneity, depends on the chosen treatment effect measure; see, for example, [5] for a discussion. An extension of the proposed method to alternative treatment effect measures may be considered in future work.

The proposed approach can also be used within the Workflow for Assessing Treatment effeCt Heterogeneity (WATCH) framework introduced by [24]. This framework emphasizes three principles: the integration of external evidence to evaluate the plausibility and relevance of subgroup findings; the use of global heterogeneity tests to assess overall departures from homogeneity; and the reliance on exploratory displays to investigate potential drivers of heterogeneity. In addition, interactive and user-friendly visualizations, such as exhaustive subgroup treatment effect plots displaying levels of evidence as discussed above, could further support decision-making by allowing stakeholders to explore subgroup patterns while simultaneously assessing their robustness against multiplicity adjustments.

Acknowledgments

The authors thank Professor Oliver Dukes for helpful comments and discussions on an earlier version of this paper.

References

- [1] M. Alos, M. F. Huque, F. Bretz, and R. B. D'Agostino Sr. Tutorial on statistical considerations on subgroup analysis in confirmatory clinical trials. *Statistics in Medicine*, 36(8):1334–1360, 2017.
- [2] C. Bonferroni. Teoria statistica delle classi e calcolo delle probabilita. *Pubblicazioni del R istituto superiore di scienze economiche e commerciali di firenze*, 8:3–62, 1936.
- [3] F. Bretz and P. H. Westfall. Multiplicity and replicability: two sides of the same coin. *Pharmaceutical Statistics*, 6(13):343–344, 2014.
- [4] A. Chakrabortty, J. Lu, T. T. Cai, and H. Li. High dimensional m-estimation with missing outcomes: A semi-parametric framework. *arXiv preprint arXiv:1911.11345*, 2019.
- [5] Y. Chen, S. Sun, K. Sechidis, C. Zhang, T. Hothorn, and B. Bornkamp. Comparing methods to assess treatment effect heterogeneity in general parametric regression models. *arXiv preprint arXiv:2503.22548, to appear in Statistics in Medicine*, 2025.
- [6] V. Chernozhukov, D. Chetverikov, M. Demirer, E. Duflo, C. Hansen, W. Newey, and J. Robins. Double/debiased machine learning for treatment and structural parameters. *The Econometrics Journal*, 21:C1 – C68, 2018.
- [7] V. Chernozhukov, M. Demirer, E. Duflo, and I. Fernández-Val. Generic machine learning inference on heterogeneous treatment effects in randomized experiments. *arXiv preprint arXiv:1712.04802*, 2017.

[8] S. R. Cole, J. K. Edwards, and S. Greenland. Surprise! *American Journal of Epidemiology*, 190(2):191–193, 07 2020.

[9] P. Ding, A. Feller, and L. Miratrix. Randomization inference for treatment effect variation. *Journal of the Royal Statistical Society Series B: Statistical Methodology*, 78(3):655–671, 2016.

[10] O. Dukes, M. J. Stensrud, R. Brioschi, and A. Hudson. Nonparametric tests of treatment effect homogeneity for policy-makers. *arXiv preprint arXiv:2410.00985*, 2024.

[11] A. Genz and F. Bretz. *Computation of Multivariate Normal and t Probabilities*. Springer, Berlin, 2009.

[12] S. Greenland. Valid p-values behave exactly as they should: Some misleading criticisms of p-values and their resolution with s-values. *The American Statistician*, 73(sup1):106–114, 2019.

[13] S. Greenland. Divergence versus decision p-values: A distinction worth making in theory and keeping in practice: Or, how divergence p-values measure evidence even when decision p-values do not. *Scandinavian Journal of Statistics*, 50(1):54–88, 2023.

[14] J. Hahn. On the role of the propensity score in efficient semiparametric estimation of average treatment effects. *Econometrica*, pages 315–331, 1998.

[15] F. Harrell. Biostatistics for biomedical research, 2025. Section 13.6 under <https://hbiostat.org/bbr/> (accessed July 29, 2025).

[16] E. H. Kennedy. Towards optimal doubly robust estimation of heterogeneous causal effects. *Electronic Journal of Statistics*, 17(2):3008–3049, 2023.

[17] E. H. Kennedy. Semiparametric doubly robust targeted double machine learning: a review. In *Handbook of statistical methods for precision medicine*, pages 207–236. Chapman and Hall/CRC, 2024.

[18] D. M. Kent, J. K. Paulus, D. Van Klaveren, R. D’Agostino, S. Goodman, R. Hayward, J. P. Ioannidis, B. Patrick-Lake, S. Morton, M. Pencina, et al. The predictive approaches to treatment effect heterogeneity (path) statement. *Annals of internal medicine*, 172(1):35–45, 2020.

[19] B. Kirsch, S. Jeske, S. Lippert, T. Schmelter, C. Muysers, and H. Kulmann. *subscreen: Systematic Screening of Study Data for Subgroup Effects*, 2022. R package version 3.0.7.

[20] C. Muysers, A. Dmitrienko, H. Kulmann, B. Kirsch, S. Lippert, T. Schmelter, A. Schulz, N. Mentenich, H. Schmitz, M. Schaefers, et al. A systematic approach for post hoc subgroup analyses with applications in clinical case studies. *Therapeutic Innovation & Regulatory Science*, 54:507–518, 2020.

[21] E. Polley, E. LeDell, C. Kennedy, and M. van der Laan. *SuperLearner: Super Learner Prediction*, 2024. R package version 2.0-29.

[22] S. J. Ruberg. Assessing and communicating heterogeneity of treatment effects for patient subpopulations: the hardest problem there is. *Pharmaceutical Statistics*, 20(5):939–944, 2021.

[23] S. Schandelmaier, M. Briel, R. Varadhan, C. H. Schmid, N. Devasenapathy, R. A. Hayward, J. Gagnier, M. Borenstein, G. J. van der Heijden, I. J. Dahabreh, X. Sun, W. Sauerbrei, M. Walsh, J. P. Ioannidis, L. Thabane, and G. H. Guyatt. Development of the instrument to assess the credibility of effect modification analyses (iceman) in randomized controlled trials and meta-analyses. *CMAJ*, 192(32):E901–E906, 2020.

[24] K. Sechidis, S. Sun, Y. Chen, J. Lu, C. Zhang, M. Baillie, D. Ohlssen, M. Vandemeulebroecke, R. Hemmings, S. Ruberg, et al. Watch: a workflow to assess treatment effect heterogeneity in drug development for clinical trial sponsors. *Pharmaceutical Statistics*, 24(2):e2463, 2025.

[25] K. Sechidis, C. Zhang, S. Sun, Y. Chen, A. Spector, and B. Bornkamp. Using individualized treatment effects to assess treatment effect heterogeneity. *Statistics in Medicine*, 44(28-30):e70324, 2025.

[26] S. Senn. Controversies concerning randomization and additivity in clinical trials. *Statistics in Medicine*, 23(24):3729–3753, 2004.

[27] S. Sun, B. Bornkamp, J. Lu, A. Mirshani, K. Sechidis, and Y. Chen. benchtm: Benchmarking heterogeneous treatment effects in clinical trials. <https://github.com/Sophie-Sun/benchtm>, 2025. R package version 0.4.1.

[28] S. Sun, K. Sechidis, Y. Chen, J. Lu, C. Ma, A. Mirshani, D. Ohlssen, M. Vandemeulebroecke, and B. Bornkamp. Comparing algorithms for characterizing treatment effect heterogeneity in randomized trials. *Biometrical Journal*, 66(1):2100337, 2024.

[29] J. D. Wallach, P. G. Sullivan, J. F. Trepanowski, K. L. Sainani, E. W. Steyerberg, and J. P. Ioannidis. Evaluation of evidence of statistical support and corroboration of subgroup claims in randomized clinical trials. *JAMA internal medicine*, 177(4):554–560, 2017.

[30] J. A. Watson and C. C. Holmes. Machine learning analysis plans for randomised controlled trials: detecting treatment effect heterogeneity with strict control of type i error. *Trials*, 21(1):156, 2020.

[31] S. Yusuf, J. Wittes, J. Probstfield, and H. A. Tyroler. Analysis and interpretation of treatment effects in subgroups of patients in randomized clinical trials. *JAMA*, 266(1):93–98, Jul 1991.

A Covariate data description for simulated, synthetic data

Table 3: Naming of baseline variables and used categories

Names	Description	Categories
AGE		(22,56], (56,66], (66,110]
ASPRNFL	Baseline Aspirin Therapy	N, Y
BASECRP		(-0.72,0.5], (0.5,0.75], (0.75,2.5]
ETHNIC		HISPANIC OR LATINO, NOT HISPANIC OR LATINO, UNKNOWN
GLYCEM	Glycemic Status at Baseline	Diabetic, Normoglycemic, Prediabetic
LBEGFG1B	Baseline EGF rate (mL/min)	< 60 mL/min/SA, >= 60 to < 90 mL/min/SA, >= 90 mL/min/SA
LBLOGHDL	Base log value of HDL cholest. (mmol/L)	(-0.89,0.0086], (0.0086,0.1], (0.1,0.59]
LBLOGLDL	Base log value of LDL-C derived (mmol/L)	(-1.7,0.26], (0.26,0.4], (0.4,1.2]
LBLOGTRI	Base log value of Triglycerides (mmol/L)	(-0.62,0.11], (0.11,0.29], (0.29,1.7]
MHGOUTFL	Medical History of Gout	N, Y
QMITGR3	Time Since Qualifying MI	< 12 months, >= 12 months
RACE		ASIAN, OTHER, WHITE
REGION1		ASIA, CENTRAL EUROPE, LATIN AMERICA, NORTH AMERICA, OTHERS, WESTERN EUROPE
SEX		F, M
SMOKE	Smoking Status at Baseline	Current smoker, Former smoker, Never
STATINB	Base median daily dose of statin (mg)	High Dose, Low Dose, Medium Dose, No Dose
VSBMIS	Screening BMI (kg/m ²)	(11,28], (28,32], (32,94]
VSSTDBMB	Baseline mean sitting diastolic BP (mmHg)	(32,74], (74,82], (82,150]
VSSTSBMB	Baseline mean sitting systolic BP (mmHg)	(120,140], (140,240], (63,120]

B Calculation of correlation across estimates

To estimate the correlation between $\widehat{\Delta}_j$, we notice that

$$Cov(\widehat{\delta}_i - \widehat{\delta}, \widehat{\delta}_j - \widehat{\delta}) = Cov(\widehat{\delta}_i, \widehat{\delta}_j) - Cov(\widehat{\delta}_i, \widehat{\delta}) - Cov(\widehat{\delta}_j, \widehat{\delta}) + Var(\widehat{\delta}),$$

where

$$\begin{aligned} Cov(\widehat{\delta}_i, \widehat{\delta}_j) &= \frac{1}{N_i N_j} Cov\left(\sum_{l \in S_i} \varphi_l, \sum_{l \in S_j} \varphi_l\right) \\ &= \frac{1}{N_i N_j} \sum_{l \in S_i \cap S_j} Var(\varphi_l) = \frac{N_{ij}}{N_i N_j} \cdot \sigma^2 \end{aligned} \quad (2)$$

Combine (2) with the formula for the covariance and variance derived in the main text we have:

$$Cov(\widehat{\delta}_i - \widehat{\delta}, \widehat{\delta}_j - \widehat{\delta}) = \frac{N_{ij}}{N_i N_j} \cdot \sigma^2 - \frac{2\sigma^2}{N} + \frac{\sigma^2}{N} = \frac{N_{ij}}{N_i N_j} \cdot \sigma^2 - \frac{\sigma^2}{N}$$

and the correlation is thus

$$Corr(\widehat{\delta}_i - \widehat{\delta}, \widehat{\delta}_j - \widehat{\delta}) = \frac{Cov(\widehat{\delta}_i - \widehat{\delta}, \widehat{\delta}_j - \widehat{\delta})}{\sqrt{Var(\widehat{\delta}_i - \widehat{\delta})Var(\widehat{\delta}_j - \widehat{\delta})}} = \frac{\frac{N_{ij}}{N_i N_j} - \frac{1}{N}}{\sqrt{(\frac{1}{N_i} - \frac{1}{N})(\frac{1}{N_j} - \frac{1}{N})}}$$

C Additional plot

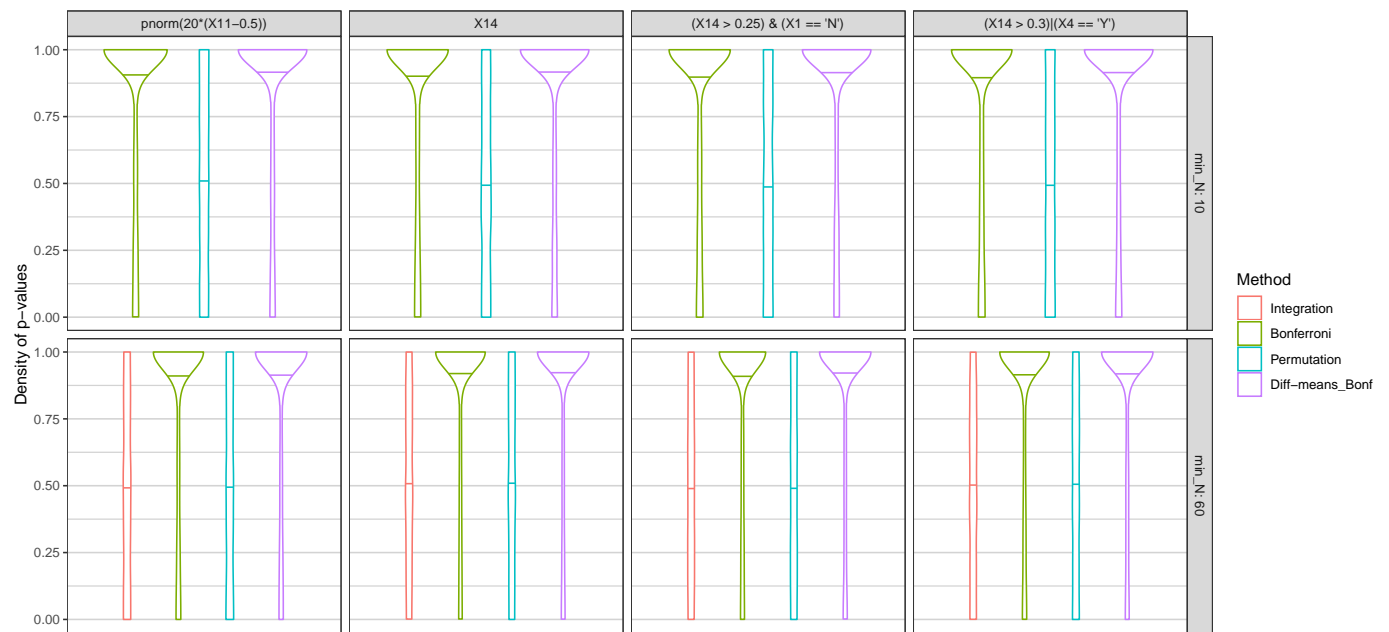


Figure 6: Distribution of p-values under homogeneous treatment effects, based on density plots, horizontal lines indicate the median.